*Desalination and Water Treatment*
www.deswater.com
doi: 10.1080/19443994.2013.808486

52 (2014) 459–469
January

Taylor & Francis
Taylor & Francis Group

# Studies on sulfonated styrene acrylonitrile and cellulose acetate blend ultrafiltration membranes

K.S. Radha[a], K.H. Shobana[b], M. Tarun[b], D. Mohan[b,*]

[a]*Department of Chemistry, R.M.D. Engineering College, Chennai, India*
[b]*Membrane Laboratory, Department of Chemical Engineering, A.C. Tech, Anna University, Chennai, India*
*Email: mohantarun@gmail.com*

Received 19 April 2012; Accepted 14 March 2013

ABSTRACT

Membranes are increasingly used in the chemical and bioprocess industries replacing more conventional separation techniques. Blending of various polymers has stimulated great interest in membrane science to improve the performance of membranes, such as hydrophilicity and flux and to reduce the fouling behavior. This paper deals with the preparation of flat-sheet asymmetric blend ultrafiltration (UF) membranes by solution casting, followed by a phase separation method. Sulfonated styrene acrylonitrile (SSAN) was selected as the hydrophilic polymer in the blend. The blend membranes were prepared with different compositions of CA and SSAN. The prepared membranes were characterized for their UF performances, such as pure water flux, water content, porosity, membrane hydraulic resistance, and morphology. The average pore size and porosity of the membranes were revealed by pore statistics and molecular weight cut-off (MWCO) studies using different molecular weight of proteins. Observations from scanning electron microscope provided qualitative evidence for the trends obtained for pore statistics and MWCO results. The membranes were also characterized for their separation performance with proteins and metal ion solutions. The rejection of proteins and metal ions was marginally decreased, whereas the permeate flux was radically improved. The polymer-enhanced UF technique has been shown to be a promising technique for removal of heavy metals in solution. In this study, the process has been investigated for removal of toxic heavy metals, such as Cu(II), Ni(II), Zn(II), and Cd(II), from synthetic wastewater solutions.

*Keywords:* Cellulose acetate; Sulfonated styrene acrylonitrile; Ultrafiltration; Molecular weight cut-off; Wastewater treatment

## 1. Introduction

Metal ions play an essential role in many biological processes and because of their competition with essential metals in binding with proteins, heavy metal ions act as potent enzyme inhibitors, exerting toxic effects on living organisms. Cadmium, copper, lead, mercury, nickel, and zinc are among the most hazardous heavy metals and extraction of these pollutants from contaminated sediments and liquid wastes is a

*Corresponding author.

*Presented at the DAE—BRNS Biennial Symposium on Emerging Trends in Separation Science and Technology (SESTEC 2012) Mumbai, India, 27 February–1 March 2012*

1944-3994/1944-3986 © 2013 Balaban Desalination Publications. All rights reserved.

task of the highest priority for the protection of the natural environment. Therefore, there is continuing interest in developing efficient methods for the selective separation and recovery of metal ions from waste waters [1,2]. Heavy metal ions, such as Cr(VI), Cu(II), Zn(II), etc., from wastewater streams could be separated and concentrated through binding of the target metal ions to water-soluble polyelectrolyte and subsequent ultrafiltration (UF) of the bound metals from the unbound components [3,4].

In the last decade, UF has become a standard procedure for the separation of macromolecular solutions. Separation of colloidal suspensions by UF can be achieved by permselective membranes, which allow the passage of solvent and small solute molecules but retain macromolecules [5,6]. The separation of proteins by membranes was found to be advantageous because of the nondestructivity and limiting denaturation of proteins in the process [7]. Intensive research has been carried out by several researchers on the transmission and rejection of proteins using cellulose acetate (CA) and polysulfone (PSf) membranes and confirmed the reliability of the process of UF in macromolecular separations [8–11].

Membrane technology has become an attractive alternative to many energy-intensive separation processes because separation using membranes do not require additives and they can be performed isothermally at low temperatures with minimum energy consumption [12]. The success of membrane technology relies on the membrane material.

Continual development of new membrane material is crucial to sustain and expand the growing interest in this technology.

CA has been considered as an important membrane material ever since the development of asymmetric membranes because of the advantages, such as moderate flux, high salt rejection properties, and renewable source of raw material. The requirement of more chemical and mechanical resistant membranes and aggressive cleaning led to the necessity of modified CA-based membranes. The hydrophilic/hydrophobic balance, as well as the physico-chemical properties of the CA membranes, can be improved by the means of blending with a suitable polymer. CA has been blended with several high-performance polymers, such as poly(sulfone), poly(ethersulfone), poly (etherimide), and styrene acrylonitrile [13], for improving the CA membrane properties and was found to be successful. A number of membranes using SAN have been made for pervaporation due to its solvent stability. Hence, SAN has been incorporated into CA to bring about desirable properties in the resultant blend membranes. This polymer pair exemplifies the use of polymer blend membrane composing with hydrophobic and hydrophilic polymers as that of polyacrylonitrile (PAN) and polyvinylchloride and CA and PSf in the literature [13].

The present study is one of our series of investigations into the preparation of sulfonated styrene acrylonitrile incorporated CA UF membranes and its characterization. This study focuses on the effects of CA/SSAN blend composition on the rejection and permeate flux of proteins, such as bovine serum albumin (BSA), egg albumin (EA), pepsin, and trypsin, and separation of toxic heavy metal ions, such as Cu(II), Ni(II), Zn(II), and Cd(II), from synthetic wastewater solutions. Polyethyleneimine (PEI) was used as the polyelectrolyte for binding with the metal ions, thereby enhancing the separation [14]. Solute rejection method has been used for determining pore statistics and MWCO and the results are discussed. The morphology of different membranes prepared with various blend compositions and additive concentrations used in the study has also been studied using scanning electron microscopy.

## 2. Experimental

### 2.1. Materials

Commercial grade CA was procured from Mysore Acetate and Chemical Co. Ltd., Mysore, India. The CA was recrystallized from acetone and then dried in a vacuum oven at 70°C for 24 h prior to use. Analar grade N,N´-dimethyl formamide (DMF) from SD Fine Chemicals, India, was used as such without further purification. Other solvents of Analar grade, such as 1,2-dichloroethane (DCE), isopropanol, N,N-dimethyl acetamide (DMAc), and acetone from SD Fine Chemicals, India, were used as such without further purification. Styrene acrylonitrile (Luran 358 N) was supplied as gift sample by the BASF, India. It was used as received. Sulfonated styrene acrylonitrile was prepared by the sulfonation of styrene acrylonitrile. Chlorosulfonic acid (AR) was procured from E. Merck Ltd. and was used as sulfonating reagent. N, N-dimethylformamide (DMF) and sodium lauryl sulfate (SLS) were obtained from Qualigens Fine Chemicals, Glaxo India Ltd., India, which were of analytical grade. DMF was sieved through molecular sieves (Type-4A°) to remove moisture and stored in dry condition prior to use. Acetone (AR) of analytical grade procured from SRL Pvt. Ltd., India, was used as such. PEI was procured from Fluka, Germany. Analytical grade copper sulfate, cobalt sulfate, zinc sulfate, and cadmium sulfate were procured from Merck

(India) Ltd. and used as received. Deionized and distilled water was employed for metal ion solutions.

### 2.2. Sulfonation of SAN

Styrene acrylonitrile (Luran 358 N) was sulfonated by chlorosulfonic acid as the sulfonating agent as reported earlier [15–17]. Twenty grams of SAN was dissolved in 100 ml of DCE at 60˚C and subsequently the SAN solution was kept at 30˚C and was placed in a three-necked, round-bottom flask. The solution was stirred using a mechanical stirrer in a nitrogen atmosphere. Then, 10 ml of chlorosulfonic acid, diluted with 200 ml of DCE, was slowly added drop-wise to the SAN solution by using a dropping funnel within one h with vigorous stirring. After being reacted for three h, the reaction product, which precipitated in the reaction medium, was dissolved in DMAc at 50˚C, coagulated with excess isopropanol, filtered, washed with isopropanol, and dried at 40˚C in a vacuum oven. The sodium salt form of the product was obtained by soaking it in excess 0.1 mol/L NaOH aqueous solution for two days. The chemical structure of SSAN is shown in Fig. 1.

### 2.3. Fabrication of blend membrane

The membranes were prepared by "phase inversion" technique employed in our earlier works as reported by other researchers. [17–19]. The casting solution was prepared by dissolving CA in DMF solvent in a round-bottom flask to which SSAN polymer was added and was subjected to constant stirring for 4 h at room temperature. The homogeneous solution thus obtained was allowed to stand at room temperature for at least six hours in an airtight condition to get rid of air bubbles and cast at room temperature by spreading them over a glass plate with the doctor blade to form a thin film of membrane.

The thickness of the membranes was maintained at $0.22 \pm 0.02$ mm and verified with a micrometer having precision of 0.01 mm. The casting and gelation conditions were kept constant throughout, since the thermodynamic conditions would largely affect the morphology and performance of the resulting membranes [20]. The gelation bath consisting of 2.5% (v/v) DMF and 0.2% (wt. basis) SLS in distilled water was prepared. The former was added to reduce the rate of liquid–liquid demixing and macrovoid formation, while the latter would reduce surface tension at the polymer–non-solvent interface. The solution after casting was exposed to atmosphere for 30 s for evaporation of solvent and immediately immersed in the coagulation bath and maintained at 18˚C. The membrane was kept undisturbed in the gelation bath for at least 1–3 h for complete precipitation and for the leaching out of the solvent from the surface of the membrane during its formation. The film casting and gelation conditions for the fabrication of CA/SSAN blend membranes given below in Table 1. Later, the membranes were removed and washed thoroughly with distilled water to remove excess DMF and surfactant and subsequently stored in 0.1 wt.% of formalin solution to avoid microbial attack [21]. The total fraction of solids in membrane formulation was held constant at 17.5 wt.% and the blend compositions of 95/5, 90/10, 85/15, /80/20, and 75/25 wt.% (CA/SSAN) of total polymer concentration in the casting solution were chosen for the preparation of CA/SSAN blend membranes. The threshold limit of the SSAN concentration was maintained to a maximum of 25 wt.% in CA polymer because beyond this concentration, there was no compatibility between the polymers.

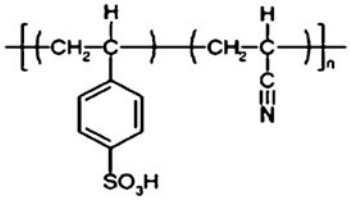


Fig. 1. Sulfonated styrene acrylonitrile.

### 2.4. Experimental setup

The synthesized membranes are characterized using a batch type dead end cell (UF Cell–S76–400-Model, Spectrum, USA) with an internal diameter of 76 mm, 450 ml capacity, holdup volume of 100 ml, and effective membrane filtration area of 38.5 $cm^2$ fitted with Teflon-coated magnetic paddle. The cell was connected to a nitrogen cylinder with the pressure control valve and gauge through a feed reservoir, and the applied pressure was 345 kPa. A constant agitation speed of 500 rpm was used throughout the study, in order to reduce the concentration polarization.

### 2.5. UF characterization

The prepared CA/SSAN membranes were characterized for compaction at a pressure of 414 kPa and the water flux was measured every 1 h for the duration of 10 min. Then, the compacted membranes were used in UF experiments in the determination of pure water flux (PWF), water content, and hydraulic resistance of the membranes [22]. Further, membrane morphology was also investigated using SEM.

#### 2.5.1. Compaction

The thoroughly washed membrane was cut into desired shape and fitted in UF kit. The distilled water was fed into the UF kit from the pressure reservoir and the initial water flux was taken after the pressurization at 414 kPa [22]. The membranes were compacted till the steady state was obtained. The compacted membranes were used in the subsequent UF experiments at 345 kPa.

#### 2.5.2. Pwf

The compacted membranes were subjected to a differential system pressure of 345 kPa and the permeate was collected. The PWF was calculated using the equation:

$$J_w = \frac{Q}{\Delta t \times A} \quad (1)$$

where $J_w$ is the PWF ($lm^{-2}h^{-1}$); $Q$ is the amount of permeates collected (l); $\Delta t$ is the sampling time (h); and $A$ is the membrane area ($m^2$).

#### 2.5.3. Water content

Water content of the membranes was obtained after soaking the membranes in water for 24 h and the membranes were weighed after mopping it with blotting paper. The wet membranes were placed in a vacuum drier at 75°C for 48 h and the dry weights were determined. The percentage of water content was calculated based on the equation:

$$\%\ \text{Water content} = \frac{\text{wet sample weight} - \text{dry sample weight}}{\text{wet sample weight}} \times 100 \quad (2)$$

#### 2.5.4. Membrane hydraulic resistance ($R_m$)

The membrane resistance is the resistance offered by the membrane to the feed flow. It is an indication of the tolerance of the membrane toward hydraulic pressure and is calculated using the equation [21]:

$$R_m = \frac{\Delta P}{J_w} \quad (3)$$

To determine membrane hydraulic resistance ($R_m$), the PWF of the membranes was measured at different transmembrane pressures ($\Delta P$), viz. 69, 138, 207, 276, and 345 kPa, after compaction. The resistance of the membrane, $R_m$, was evaluated from the slope obtained by plotting water flux vs. transmembrane pressure difference ($\Delta P$) (Table 1).

#### 2.5.5. Protein separation studies

Protein solutions of BSA, EA, pepsin, and trypsin were prepared (0.1 wt.%) in phosphate buffer (0.5 M, pH 6.0) and used as a standard solution for the rejection studies. Filtration through each membrane was carried out individually and the concentration of the feed solution was kept constant throughout the run. The permeate protein concentration collected over different time intervals was estimated using UV–visible spectrophotometer (Hitachi, model U-2000) at a wavelength of 280 nm. The percentage of protein rejection was calculated from the concentration of the feed and the permeate using the Eq. (4):

$$\%SR = 1 - \frac{C_p}{C_f} \times 100 \quad (4)$$

where $C_f$ and $C_p$ are the concentration of protein in the feed and permeate solution, respectively.

The protein solution permeate flux is determined as follows [23]:

$$J_w = \frac{Q}{\Delta t \times A} \quad (5)$$

where $J_w$ is the protein flux (in $1\,m^{-2}h^{-1}$); $Q$ is the quantity of protein permeate in liters; $\Delta t$ is the sampling time (in h); and $A$ is the membrane area (in $m^2$).

#### 2.5.6. Molecular weight cut-off (MWCO)

MWCO and pore size of the prepared membranes were calculated by performing sieving experiments with dilute protein solutions of different molecular weights [24]. The MWCO has a linear relationship

Table 1
Film-casting and gelation conditions for the CA/SSAN blend membranes

| | |
|---|---|
| Casting solution temperature | 42 ± 2°C |
| Casting temperature | 25 ± 1°C |
| Casting relative humidity | 50 ± 2% |
| Solvent evaporation time | 30 s |
| Temperature of the gelation bath (°C) | 10–14 |
| Period of gelation (h) | >12 |
| Thickness of the membrane (mm) | 0.18–0.22 |

with the pore size of the membrane. In general, the MWCO of the membrane is determined by identifying an inert molecule of lowest molecular weight that has a solute rejection of more than 80% in steady-state UF experiments. MWCO of individual membranes was calculated by the values obtained from the knowledge of rejection percent of different proteins by CA.

#### 2.5.7. Pore statistics

From the protein rejection studies, the average pore radius, surface porosity, and pore density of the membrane were calculated. The average pore radius was found from percent of solute rejection and $\varepsilon$ calculated using the equation:

$$\overline{R} = \frac{\overline{\alpha}}{\%\mathrm{SR}} \times 100 \tag{6}$$

where $\overline{R}$ is the average pore radius ($\overset{0}{A}$) of the membrane; $\overline{\alpha}$ is the average solute radius ($\overset{0}{A}$); and is constant for each molecular weight. The average solute radii is known as "stoke radii" and the value of $\overline{\alpha}$ can be found from the plot between the solute radius and molecular weight of the solute given by Sarbolouki [25], which is shown in Table 2.

The surface porosity, $\varepsilon$, of the membrane was calculated by the orifice model given below assuming that only the skin layer of the membrane is effective in separation [26]:

$$\varepsilon = \frac{3\pi\eta_{\mathrm{w}} J_{w1}}{R \times \Delta \mathrm{P}} \tag{7}$$

where $\varepsilon$ is the surface porosity; $\eta_w$ is the velocity of the deionized water (g/cm s); $J_{w1}$ is the PWF (cm/s); and $\Delta P$ is the applied pressure (dyn/cm$^2$). From the known values of $\varepsilon$ and $\overline{R}$ (in cm), the pore density in the membrane surface can be calculated using equation

$$n = \frac{\varepsilon}{\pi \times \overline{R}^2} \tag{8}$$

where $n$ is number of pores/cm$^2$.

#### 2.5.8. Metal-ion rejection

Synthetic wastewater solutions of $Cu^{2+}$, $Ni^{2+}$, $Zn^{2+}$, and $Cd^{2+}$ with an approximate 1,000 ppm concentration were prepared in 1 wt.% solution of PEI in deionized water. The pH of these aqueous solutions was adjusted to 6.25 by adding a small amount of either 0.1 M HCl or 0.1 M NaOH. Solutions containing PEI and individual metal ions or metal chelates were thoroughly mixed and left standing for five days to complete binding [27,28].

The PEI and metal ions containing solutions were filled in the feed reservoir. For each run, the first few ml of the permeate was discarded. The permeate flux was measured by collecting the permeate at a pressure of 345 kPa. The concentration of each metal ion in feed and permeate was measured by using atomic absorption spectrophotometer (Perkin Elmer-2380). The pH of feed and permeate were measured with Elico pH meter. In the absence of metal ions, the concentration of PEI was also confirmed by UV–visible Spectrophotometer (Hitachi, model U-2000) at $\lambda_{\max} = 269$ nm.

#### 2.5.9. Morphological studies

The cross-sectional images of the CA and CA/SSAN blend membranes were taken by scanning electron microscope (LEICA Stereoscan, Cambridge, UK). The membranes were cut into small pieces and cleaned with blotting paper. The pieces were immersed in liquid nitrogen for 60–90 s and were frozen. These frozen fragments of the membranes were stored in a desiccator. The dried samples were gold-sputtered for producing electric conductivity and photographs were taken in very high vacuum

Table 2
Characterization of the CA/SSAN blend membranes

| Blend composition (%) (17.5 wt.%) CA | SSAN | PWF at 345 kPa ($\mathrm{lm^{-2}\,h^{-1}}$) | Membrane hydraulic resistance $R_m$, ($\mathrm{kPa/lm^{-2}\,h^{-1}}$) | Water content (%) | Average membrane radius $R$, (Å) | Surface porosity $\varepsilon \times 10$–5 | MWCO (kDa) |
|---|---|---|---|---|---|---|---|
| 100 | 0 | 4.7 | 34.13 | 76.67 | 26.88 | 1.73 | 20 |
| 95 | 5 | 15.6 | 24.39 | 78.90 | 41.30 | 2.51 | 45 |
| 85 | 15 | 24.6 | 18.38 | 80.23 | 47.85 | 4.33 | 69 |
| 75 | 25 | 34.2 | 11.53 | 82.35 | 65.25 | 5.17 | 69 |

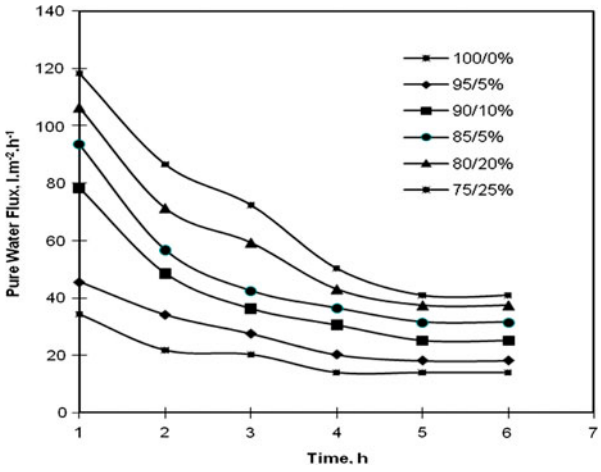


Fig. 2. Effect of compaction time on PWF of CA/SSAN blend membranes.

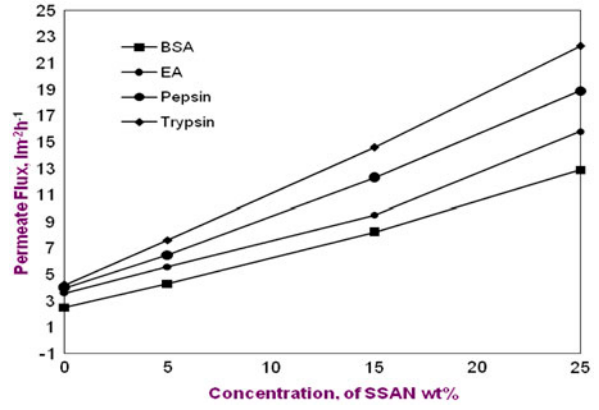


Fig. 3. Effect of concentration of SSAN on protein permeate flux.

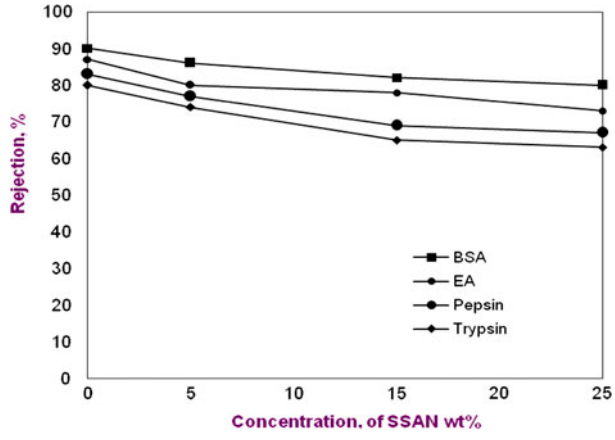


Fig. 4. Effect of concentration of SSAN on protein rejection.

operating conditions between 15 and 25 kV, depending on the physical nature of the sample.

## 3. Results and discussion

### 3.1. Compaction

In this investigation, CA was modified by blending with SSAN at varying composition from 0 to 25 wt.%. The effect of SSAN on blend membranes can be visualized from Fig. 2, where the graph is plotted between compaction time vs. PWF of blend membranes. The initial flux that was collected after 20 s of pressurization showed a value of 34.3 $lm^{-2}h^{-1}$ for 100 wt.% CA. As the compaction time increased, the value of PWF decreased to 14.0 $lm^{-2}h^{-1}$ after five h and attained the steady-state value, which confirms the completion of the compaction process. This is due to the fact that during compaction of membrane under pressure, reorganization of polymeric chains occurs which leads to the change in the membrane structure with the formation of uniform pores.

When the concentration of SSAN particle added to CA increased from 0 to 25 wt.%, the initial flux was increased from 34.3 to 118.3 $lm^{-2}h^{-1}$. This increase in trend may be due to the increased free volume between CA and SSAN in the polymer matrix, which resulted in the formation of pores on the membrane surface. Similar results were obtained by Nagendran et al. [19]. The steady-state flux of 100 wt.% CA and 25 wt.% SSAN in the CA blend membrane resulted in an increased value from 14.0 to 49.0 $lm^{-2}h^{-1}$ Arthanareeswaran et al. [29] reported similar steady-state observations. It is believed to form uniform, rigid pores during compaction on the membrane surface

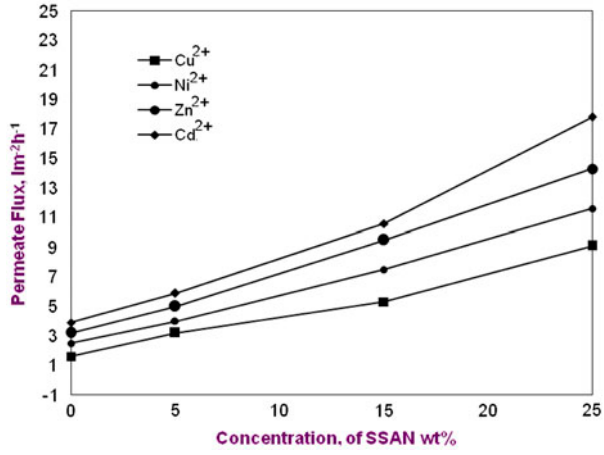


Fig. 5. Effect of concentration of SSAN on metal permeate flux.

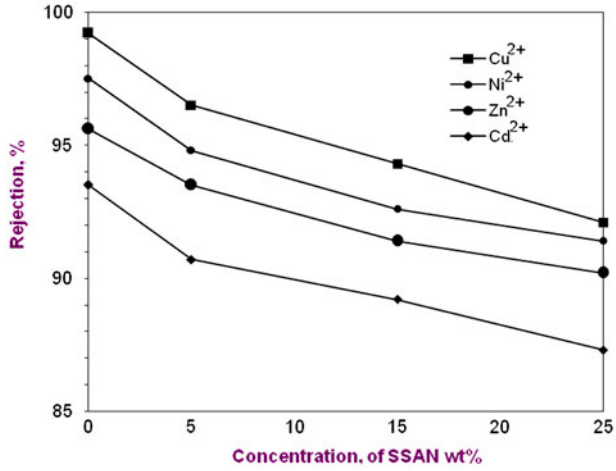


Fig. 6. Effect of concentration of SSAN on metal ion rejection.

and to obtain a steady-state flux. Similar trend was obtained for the membranes with varying compositions of 95/5, 90/10, 85/15, 80/20, and 75/25 wt.% of CA/SSAN blend composition.

### 3.2. PWF

After the completion of compaction, the PWF of blend membranes was studied at 345 kPa pressure and shown in Table 2. The low PWF value of 4.7 $lm^{-2}h^{-1}$ is obtained for 100 wt.% CA membranes. This is because for pure 100 wt.% CA, a very tight polymer matrix is formed; thus, the pores formed on the membrane surface will be in smaller size. When the concentration of SSAN is increased from 10 to 25 wt.% in the pure CA blend membrane, the PWF showed an increased value from 19.8 to 34.2 $lm^{-2}h^{-1}$. The addition of SSAN in blend not only increases the hydrophilicity of blend, but also enlarges the pore size of membranes. The effect of relative increase in pore size outweighs that of hydrophilicity, and hence increases the flux at higher SSAN composition. Similar trends were also reported by Malaisamy et al. [30].

### 3.3. % Water content

Water content of the membrane relates the hydrophilicity of the membrane [31]. The water content percent was calculated using Eq. (2) and the value of the membranes are shown in Table 2. From Table 2, the water content percent of 100 wt.% CA membrane showed a value of 76.67%. In case of 75/25 wt.% of CA/SSAN blend membrane, the water content percent was 82.35%. When 25 wt.% SSAN particles was present in the CA membrane, the water content of the blend membrane was increased. Similar increase in water content was interpreted by Hwang et al. [32]. This trend is due to the electrostatic repulsion between the polymers which restricts the polymer chain from coming close to each other increasing the void volume. Moreover, the thermo-dynamical incompatibility between the polymers further impedes the chain from coming close to each other. Further, this leads to increase in void volume, resulting in the formation of bigger size pores on the membrane surface and increases the water uptake in the pores.

### 3.4. Membrane hydraulic resistance ($R_m$)

In order to determine the membrane hydraulic resistance, the PWF was measured by varying the transmembrane pressure of the system to 414, 345, 276, 207, 138, and 69 kPa. The value of $R_m$ is calculated by Eq. (3), which reveals the resistance offered by the membrane to the feed flow. From Table 2, it is evident that the pure 100 wt.% CA exhibited a higher value of 34.13 kPa/$lm^{-2}h^{-1}$ due to low porosity of the CA membrane. In the CA/SSAN blend membranes, when the concentration of SSAN increased with 5 wt.% increments to a maximum of 25 wt.% in the casting solution, $R_m$ value gradually decreased to 11.53 kPa/$lm^{-2}h^{-1}$. The introduction of SSAN in the polymer chains is expected to be effective in promoting interface void formation during the membrane preparation. The enhanced pore size of the CA/SSAN membrane due to the extended free volume between polymer chains by the addition of SSAN resulted in the decrease of $R_m$ value as pointed out by Bottino et al. [33]. Similar decrease in $R_m$ values was obtained for other blend membranes with varying compositions of CA/SSAN, such as 95/5, 90/10, 85/15, 80/20, and 75/25 wt.%.

### 3.5. MWCO

The MWCO of a membrane corresponds to the molecular weight of solutes that has a rejection of more than 80% [25]. MWCO of all the membranes of varying composition of CA/SSAN was determined individually based on the study of protein rejection using proteins of different molecular weight and tabulated in Table 2. MWCO of the 100 wt.% CA is compared with the blend membranes with compositions of 95/5, 85/15, and 75/25 wt.% of CA/SSAN. It is evident from Table 2 that the MWCO of the pure 100 wt.% CA membrane is 20 kDa. This is because the membrane formed of pure CA has smaller pore size

due to the tight polymer matrix. Malaisamy et al. [30] obtained similar results for CA/sulfonated PSf blend membranes. When considering the MWCO of the newly formed blend membrane of 90/10 wt.%, CA/SSAN showed a higher value of 45 kDa. With the further increase of 25 wt.% SSAN to CA membrane, the MWCO further increased to 69 kDa. The increase in MWCO of the blend membranes may be due to the increase in free volume and a decrease in polymer chain segmental mobility by the presence of silica material in the polymer casting solution [34].

### 3.6. Pore statistics

Pore statistics includes average membrane pore radius (Å), surface porosity, and pore density. Average pore radius ($R$) of the membrane is found from the solute rejection percent using the protein solutions prepared from trypsin, pepsin, EA, and BSA of 0.1 wt.% in phosphate buffers. The pure 100 wt.% CA membrane was compared with the CA/SSAN blend composition of 95/5, 90/10, 85/15, 80/20, and 75/25 wt.%. It is observed that for pure 100% CA, the value of $R$ is found to be 26.88 Å. The relation between the average membrane pore radius and the concentration of SSAN in CA is given in Table 2 and it can be observed that the membrane average pore radius is 65.25Å when the concentration of SSAN is increased to 25 wt.% in the CA membrane. Surface porosity ($\varepsilon$) given in Table 2 gives details about the total pore area per unit surface area of the membrane and is calculated using Eq. (6). The value of $\varepsilon$ is found to be $1.23 \times 10^{-5}$ when the concentration of SSAN is 0 wt.% in CA membrane, which is observed from Table 2. The $\varepsilon$ value showed a comparatively higher value of $5.17 \times 10^{-5}$ for 75/25 wt.% CA/SSAN blend membrane. It was concluded that SSAN yield more polymer/polymer interfacial area and provide more opportunity to disrupt polymer chain packing.

### 3.7. Morphological studies

The SEM images were taken after testing the compaction studies of CA and CA/SSAN blend membranes. SEM micrographs of top surface and cross-section of membranes, prepared from 100% CA, are shown in Figs. 7(a)–(d). Figs. 7(a, c) depict a porous layer with a uniform pore size distribution on the top surface of membranes prepared with pure CA and 75/25 wt.% CA/SSAN. Further, the number of pores is less in 100% CA in Fig. 7(a) when compared to 75/25 wt.% CA/SSAN membrane (Fig. 7(c)). The

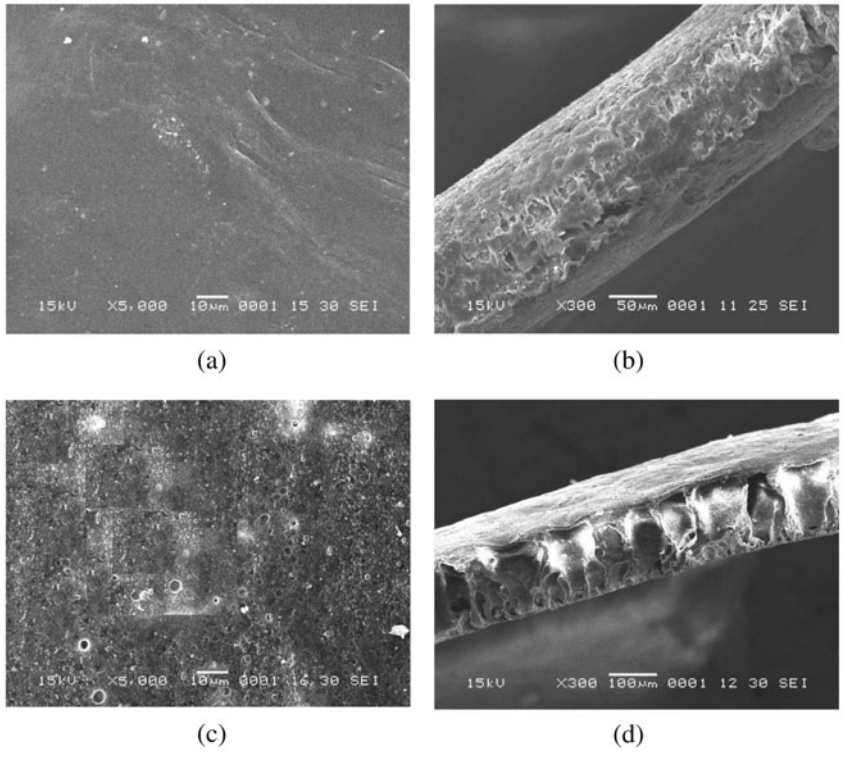


Fig. 7. Sem micrographs of CA/SSAN membranes: Top surface (5,000×): (a) 100 wt.% CA, (c) 75/25 wt.% CA/SSAN: Cross section (300×): (b) 100 wt.% CA (d) 75/25 wt.% CA/SSAN.

finger-like structures shown in Figs. 7(b, d) are the cross-sections of the above-mentioned respective membranes. Similar finger-like structures are reported [35] in the case of CA-inorganic salt membranes. A comparison of Figs. 7(b)–(d) clearly shows that the increase in pore size and finger-like voids is only due to the increase in the polymer composition from 0 to 25 wt.%. These SEM results confirm the effect of polymer composition on PWF, water content, and hydraulic resistance of the CA/SSAN blend membranes. This may be attributed to the distribution of individual domains of SSAN and CA with their respective morphologies. The cross-sectional views of CA/SSAN of the blend membranes have finger-like structures commonly found beneath the skin layer of UF membranes. The large macrovoids extend through most of the substructure, the medium-sized macrovoids extend through one-third of the membrane, and the small macrovoids are situated near the nodular layer. The skin becomes porous and a spongy structure is observed along the bottom of the penetrating cavity.

### 3.8. Separation of the protein solution

#### 3.8.1. Effect of the concentration of SSAN on the permeate flux

The effects of the concentration of SSAN on the protein solution permeate flux through various CA/SSAN blend membranes is shown in Fig. 3. It was apparent that the permeate flux of a given protein through the CA/SSAN blend membranes was higher than that through the pure CA membrane. As the SSAN concentration increased in the casting solution, the permeate flux for all of the proteins increased. The permeate flux of trypsin for the pure CA membrane was found to be $4.2 \times 10^{-6}\,m^3\,m^{-2}s^{-1}$ and for the membrane prepared from the casting solution having 40 wt.% SSAN, the permeate flux increased to $22.3 \times 10^{-6}\,m^3\,m^{-2}s^{-1}$. This was because as the concentration of SSAN in the casting solution increased, the porosity of the membranes also increased [36]. Similar trends were observed for the pepsin, EA, and BSA protein solutions. SSAN is a charged hydrophillic polymer; it is possible that electrostatic repulsion will hold up the bundling of polymers, which could give rise to larger pores or interconnected pores. Therefore, the systematic addition of SSAN could be expected to greatly increase the pore size, as we found experimentally. We observed that the permeate flux increased rapidly for all of the proteins when the concentration of SSAN increased from 15 to 25 wt.% in the casting solution. This was in agreement with the morphological structure and PWF results for the increase in concentration of SSAN from 15 to 25 wt.% in comparison to other systematic increases, as shown in Table 2. The order of magnitude of permeate flux of the protein solutions was found to be trypsin>pepsin>EA>BSA for all of the membranes; this was due to the differences in the molecular weights. The lowest permeate flux was observed for BSA at a 0 wt.% SSAN concentration, which was $2.5 \times 10^{-6}\,m^3\,m^{-2}s^{-1}$.

#### 3.8.2. Effect of the concentration of SSAN on rejection

The effects of the concentration of SSAN on the percentage rejection of proteins for all of the CA/SSAN blend membranes are shown in Fig. 4. In general, an increase in the concentration of SSAN resulted in a decrease in the percentage rejection of all of the proteins. The rejection of trypsin for the pure CA membrane was found to be 80%, whereas for the membranes prepared from the casting solutions having 5–25 wt.% SSAN, the rejection decreased up to 63%. Similar trends were observed for the rejection of pepsin, EA, and BSA. The decreasing trend of rejection as the concentration of SSAN increased was due to the fact that the porosity of the membrane increased as the concentration of SSAN in the casting solution increased, as revealed by the morphology and other results. Interestingly, the extent of rejection was on the order of BSA>EA>pepsin>trypsin for all of the membranes. This was because BSA had a higher molecular weight compared to the other three proteins, and trypsin had a lower molecular weight compared to BSA, EA, and pepsin. In general, it seemed that the observed trend was reverse for the permeate flux of the proteins.

### 3.9. Removal of metal ions

#### 3.9.1. Effect of the concentration of SSAN on the permeate flux

The permeate flux values of the synthetic metal-ion wastewater solutions on increasing concentrations of SSAN in the CA/SSAN blend membranes are shown in Fig. 5. The permeate flux values of all of the metal ions increased, as the concentration of SSAN increased in the casting solution. The permeate flux of Cu(II) for the pure CA membrane was $1.6 \times 10^{-6}\,m^3\,m^{-2}s^{-1}$, whereas for the membrane prepared from the casting solution having 25 wt.% SSAN the permeate flux increased to $9.1 \times 10^{-6}\,m^3\,m^{-2}s^{-1}$. There was a rapid increase in the permeate flux of all of the metal ions as the concentration of SSAN in the casting solution increased beyond 15 wt.%, as observed during protein-removal studies. The

permeate flux of Cu(II) was lower than those of the other metal-ion solutions and the order of the permeate flux was Cd(II)>Zn(II)>Ni(II)>Cu(II). This was because Cu(II) had a higher affinity for Ndonor ligands, compared to Cd(II) and Zn(II) [37,38]. Hence, it was possible that Cu(II) could have easily formed more macromolecules than other metal ions chosen in this study. This led to the reduced permeate flux for Cu(II) and enhanced the rejection. Hence, the extent of removal of the metal ion from the synthetic wastewater solutions depended on the formation of macromolecules with the PEI complexing agent and on the morphological structure of the membranes.

#### *3.9.2. Effect of the concentration of SSAN on rejection*

The effects of the concentration of SSAN on the rejection percent of metal ions from synthetic wastewater solutions for the CA/SSAN blend membranes are shown in Fig. 6. In general, permeate flux and rejection possess an inverse relationship, as seen in protein-removal studies. Similar to the observations made in the protein-rejection studies, the increase in the concentration of SSAN resulted in a decrease in the rejection of all of the metal ions. The rejection of Cu(II) for the pure CA membrane was 99.2% and for the membrane prepared from a casting solution having 25 wt.% SSAN, the rejection decreased to 92.1%. The rejection of Cd(II) for the pure CA membrane was 93.5%, and this value was lower than that of Cu(II). Similar observations were also found for the rejection of other metal ions, such as Zn(II) and Ni(II). The rejection of Cu(II) was found to be higher than that of other metal ions for all of the membranes, and the order of rejection was Cu(II)>Ni(II)>Zn(II)>Cd(II). This may have been due to the higher binding ability of Cu(II) with PEI. It has been shown that Cu(II) has a higher complexation constant, compared to Zn(II) and Cd(II) [39–41]. Furthermore, it is known that Zn(II) and Cd(II) complexes have low ligand–field stability because of the complete filling of d orbitals. Similar observations were reported by Mandel and Leyte [42]. Similar observations on the higher rejection of Cu(II), compared to Zn(II)>Co(II)>Cd(II) with PEI as a complexing agent, were reported by Arthanareeswaran et al. [29].

## 4. Conclusion

In this study, CA as a base polymer was blended with SSAN contents ranging from 0 to 25 wt.% with DMF as the solvent, to prepare modified CA membranes. Polymer solutions having SSAN concentrations greater than 25 wt.% did not form membranes. The characterization of the prepared membranes illustrated that the PWF and water content increased, whereas the membrane hydraulic resistance decreased as the concentration of SSAN in the casting solution increased. The SEM study showed a continuous increase in the pore size in the support layer and a subsequent decrease in the thickness of the skin layer as the concentration of SSAN in the casting solution increased, which was supported by the porosity data. The rejection of proteins was on the order BSA>EA>pepsin>trypsin, which was directly proportional to the molecular weights of the proteins. The extent of rejection of metal ions from the synthetic wastewater solutions followed the order Cu(II)>Ni(II)>Zn(II)>Cd(II), which depended on the complexation ability to form macromolecules and ligand–field stability of the individual metal ions. The results suggest that both the protein and metal-ion removal involved a sieving mechanism influenced by the molecular weight of the solute and the porosity of the membranes. The blending of SSAN with the CA polymer matrix resulted in substantially high permeability and a reduction in the membrane resistance properties; this led to a significant improvement in the flux and a marginal reduction in the rejection.

## Acknowledgment

The authors express their gratitude to BASF Limited for the gift sample of Styrene acrylonitrile used for the preparation of blend membranes.

## References

[1] M. Bodzek, I. Korus, K. Loska, Application of the hybrid complexation–ultrafiltration process for removal of metal ions from galvanic wastewater, Desalination 121 (1999) 117–121.
[2] M.M. Naim, H.E.M. Abdel Razek, Chelation and permeation of heavy metals using affinity membranes from cellulose acetate–chitosan blends, Desalin. Water Treat. 51 (2013) 644–657.
[3] K. Volchek, E. Krentsel, Y. Zhilin, G. Shtereva, Y. Dytnersky, Polymer binding/ultrafiltration as a method for concentration and separation of metals, J. Membr. Sci. 79 (1993) 253–272.
[4] I. Frenzel, D.F. Stamatialis, M. Wessling, Water recycling from mixed chromic acid waste effluents by membrane technology, Separ. Purif. Technol. 49 (2006) 76–83.
[5] R.W. Baker, H. Strathmann, Ultrafiltration of macromolecular solutions with high flux membranes, J. Appl. Polym. Sci. 14 (1970) 1197–1214.
[6] R. Lacey, S. Loeb, Industrial Membrane Technology, Wiley-Interscience, New York, 1971, pp. 134–139.
[7] A. Nagendran, D. Lawrence Arockiasamy, D. Mohan, Cellulose acetate and polyetherimide blend ultrafiltration membranes, I: Preparation, characterization, and application, Mater. Manufact. Proc. 23 (2008) 311–319.
[8] S. Nakatsuka, A.S. Michaels, Transport and separation of proteins by ultra-filtration through sorptive and nonsorptive membranes, J. Membr. Sci. 69 (1992) 189–211.

[9] W.S. Opong, A.L. Zydney, Hydraulic permeability of protein layers deposited during ultrafiltration, J. Colloid. Interf. Sci. 142 (1991) 41–60.
[10] E. Iritani, Y. Mukai, T. Murase, Upward dead-end ultrafiltration of binary protein mixtures, Sep. Sci. Technol. 30 (1995) 369–382.
[11] R. Chan, V. Chen, M.P. Bucknall, Ultrafiltration of protein mixtures: Measurement of apparent critical flux, rejection performance, and identification of protein deposition, Desalination 146 (2002) 83–90.
[12] G.M. Geise, H.S. Lee, D.J. Miller, B.D. Freeman, J.E. Mcgrath, D.R. Paul, Water purification by membranes: The role of polymer science, J. Polym. Sci. Part B: Polym. Phys 48 (2010) 1685–1718.
[13] K.S. Radha, K.H. Shobana, D. Mohan, Synthesis and characterization of styrene-acrylonitrile copolymer blend ultrafiltration membranes, Desalin. Water Treat. 12 (2009) 114–126.
[14] F.M. Almutairi, P.M. Williams, R.W. Lovitt, Effect of membrane surface charge on filtration of heavy metal ions in the presence and absence of polyethylenimine, Desalin. Water Treat. 42 (2012) 131–137.
[15] A. Nagendran, S. Vidya, D. Mohan, Preparation and characterization of cellulose acetate-sulfonated poly(etherimide) blend ultrafiltration membranes and their applications, Soft Mater. 6 (2008) 45–64.
[16] L.-Q. Shen, Z.-K. Xu, Z.-M. Liu, Y.-Y. Xu, Ultrafiltration hollow fiber membranes of sulfonated polyetherimide/polyetherimide blends: Preparation, morphologies and anti-fouling properties, J. Membr. Sci. 218 (2003) 279–183.
[17] R. Malaisamy, R. Mahendran, D. Mohan, Cellulose acetate and sulfonated polysulfone blend ultrafiltration membranes. II. Pores statistics, molecular weight cutoff, and morphological studies, J. Appl. Polym. Sci 84 (2002) 430–444.
[18] S.A. Ahmed, M.H. Sorour, H.A. Talaat, S.S. Ali, Functional analysis of cellulose acetate flat membranes prepared via casting technique, Desalin. Water Treat. 21 (2010) 115–121.
[19] A. Nagendran, A. Vijayalakshmi, D. Lawrence Arockiasamy, K.H. Shobana, D. Mohan, Toxic metal ion separation by cellulose acetate/sulfonated poly(ether imide) blend membranes: Effect of polymer composition and additive, J. Hazard. Mater. 155 (2008) 477–485.
[20] M. Sivakumar, A.K. Mohanasundaram, D. Mohan, K. Balu, R. Rangarajan, Modification of cellulose acetate: Its characterization and application as an ultrafiltration membrane, J. Appl. Polym. Sci. 67 (1998) 1939–1946.
[21] Y.Q. Wang, Y.L. Su, Q. Sun, X.L. Ma, Z.Y. Jiang, Generation of anti-biofouling ultrafiltration membrane surface by blending novel branched amphiphilic polymers with polyethersulfone, J. Membr. Sci. 286 (2006) 228–236.
[22] L. Zeman, M. Wales, Steric rejection of polymeric solutes by membranes with uniform pore size distribution, Separ. Sci. Technol. 16 (1981) 275–290.
[23] A. Vijayalakshmi, D. Lawrence Arockiasamy, A. Nagendran, D. Mohan, Separation of proteins and toxic heavy metal ions from aqueous solution by CA/PC blend ultrafiltration membranes, Separ. Purif. Technol. 62 (2008) 32–38.
[24] D. Mockel, E. Staude, M.D. Guiver, Static protein adsorption, ultrafiltration behavior and cleanability of hydrophilized polysulfone membranes, J. Membr. Sci. 158 (1999) 63–75.
[25] M.N. Sarbolouki, General Diagram for estimating pore size of UF and RO membranes, Sep. Purif. Technol. 17 (1982) 228–386.
[26] O. Velicangil, J.A. Howell, Estimation of the properties of high-flux ultrafiltration membranes, J. Phys. Chem. 84 (1980) 2991–2992.
[27] N.V. Jarvis, J.M. Wagener, Mechanistic studies of metal ion binding to water soluble polymers using potentiometry, Talanta 12 (1995) 219–226.
[28] C. Cifci, O. Durmaz, Removal of heavy metal ions from aqueous solutions by poly(methyl m ethacrylate-co-ethyl acrylate) and poly(methyl methacrylate-co-buthyl m ethacrylate) membranes, Desalin. Water Treat. 28 (2011) 255–259.
[29] G. Arthanareeswaran, P. Thanikaivelan, M. Raajenthiren, Sulfonated poly(ether ether ketone)-induced porous poly (ether sulfone) blend membranes for the separation of proteins and metal ions, J. Appl. Polym. Sci. 116 (2010) 995–1004.
[30] R. Malaisamy, R. Mahendran, D. Mohan, M. Rajendran, V. Mohan, Cellulose acetate and sulfonated polysulfone blend ultrafiltration membranes. I. Preparation and characterization, J. Appl. Polym. Sci. 86 (2002) 1749–1761.
[31] M. Sivakumar, D. Mohan, R. Rangarajan, Studies on cellulose acetate polysulfone ultrafiltration membranes II. Effect of additive concentration, J. Membr. Sci. 268 (2006) 208–219.
[32] J.R. Hwang, S. Koo, S. Koo, J.H. Kim, A. Higuchi, T. Tak, Effects of casting solution composition on performance of poly(ether sulfone) membrane, J. Appl. Polym. Sci. 60 (1996) 1343–1348.
[33] A. Bottino, G. Capannelli, A. Imperato, S. Munari, Ultrafiltration of hydrosoluble polymers: Effect of operating conditions on the performance of the membrane, J. Membr. Sci. 21 (1984) 247–267.
[34] C.J. Cornelius, E. Marand, Hybrid silica-polyimide composite membranes: Gas transport properties, J. Membr. Sci. 202 (2002) 97–118.
[35] C. Lemoyne, C. Friedrich, J.L. Halary, C. Noel, L. Monnerie, Physicochemical processes occurring during the formation of cellulose diacetate membranes. Research of criteria for optimizing membrane performance. V. Cellulose diacetate- acetone-water-inorganic salt casting solutions, J. Appl. Polym. Sci. 25 (1980) 1883–1913.
[36] W.R. Bowen, T.A. Doneva, H.B. Yin, Polysulfone — sulfonated poly(ether ether) ketone blend membranes: Systematic synthesis and characterization, J. Membr. Sci. 181 (2001) 253–263.
[37] A.J. Blake, A. Bencini, C. Caltagirone, G.D. Filippo, L.S. Dolci, A. Garau, F. Isaia, V. Lippolis, P. Mariani, L. Prodi, M. Montalti, N. Zaccheroni, C.A. Wilson, A new pyridine-based 12-membered macrocycle functionalised with different fluorescent subunits; coordination chemistry towards Cu(II), Zn(II), Cd(II), Hg(II), and Pb(II), *Dalton Trans*. (2004) 2771–2779.
[38] C. Çifci, O. Şanlı, Poly(vinyl pyrrolidone)-enhanced crossflow filtration of Fe(III), Cu(II) and Cd(II) ions using alginic acid/cellulose composite membranes, Desalin. Water Treat. 29 (2011) 87–95.
[39] C. Bazzicalupi, P. Bandyopadhyay, A. Bencini, A. Bianchi, C. Giorgi, B. Valtancoli, D. Bharadwaj, P.K. Bharadwaj, R.J. Butcher, Complexation properties of heteroditopic cryptands towards Cu(II), Zn(II), Cd(II) and Pb(II) in aqueous solution: Crystal structures of $[H_5L1]$ $(ClO)_5.4H_2O$ and [NiL2(Cl)] Cl.5.5$H_2$O.MeOH, Eur. J. Inorg. Chem. 6 (2000) 2111–2116.
[40] F.M. Almutairi, P.M. Williams, R.W. Lovitt, Polymer enhanced membrane filtration of metals: Retention of single and mixed species of metal ions based on adsorption isotherms, Desalin. Water Treat. 28 (2011) 130–136.
[41] C. García, E. Rogel-Hernández, G. Rodríguez, F. Wakida, E. Vélez, H. Espinoza-Gómez, Natural organic matter removal from water by complexation-ultrafiltration process with poly (diallyl dimethylammonium chloride), Desalin. Water Treat. 22 (2010) 17–21.
[42] M. Mandel, J.C. Leyte, Interaction of poly(methacrylic acid) and bivalent counterions. I. J. Polym. Sci. Part A: Gen Pap 2 (1964) 2883–2899.